Erschienen in: Journal of Bacteriology ; 193 (2011), 23. - S. 6760-6769

Cyclohexane-1,2-Dione Hydrolase from Denitrifying *Azoarcus* sp. Strain 22Lin, a Novel Member of the Thiamine Diphosphate Enzyme Family

Alma K. Steinbach,[1] Sonja Fraas,[1] Jens Harder,[2] Anja Tabbert,[1] Henner Brinkmann,[1,3] Axel Meyer,[1] Ulrich Ermler,[4] and Peter M. H. Kroneck[1]*

Fachbereich Biologie, Universitaet Konstanz, 78457 Constance, Germany[1]; Department of Microbiology, Max-Planck-Institute for Marine Microbiology, Celsiusstr. 1, 28359 Bremen, Germany[2]; Département de Biochimie, Faculté de Médecine, Université de Montréal C.P. 6128, Succ. Centre-Ville, Montréal, Quebec H3C 3J7, Canada[3]; and Max-Planck-Institut für Biophysik, Max-von-Laue-Str. 3, 60438 Frankfurt, Germany[4]

Alicyclic compounds with hydroxyl groups represent common structures in numerous natural compounds, such as terpenes and steroids. Their degradation by microorganisms in the absence of dioxygen may involve a C—C bond ring cleavage to form an aliphatic intermediate that can be further oxidized. The cyclohexane-1,2-dione hydrolase (CDH) (EC 3.7.1.11) from denitrifying *Azoarcus* sp. strain 22Lin, grown on cyclohexane-1,2-diol as a sole electron donor and carbon source, is the first thiamine diphosphate (ThDP)-dependent enzyme characterized to date that cleaves a cyclic aliphatic compound. The degradation of cyclohexane-1,2-dione (CDO) to 6-oxohexanoate comprises the cleavage of a C—C bond adjacent to a carbonyl group, a typical feature of reactions catalyzed by ThDP-dependent enzymes. In the subsequent NAD^+-dependent reaction, 6-oxohexanoate is oxidized to adipate. CDH has been purified to homogeneity by the criteria of gel electrophoresis (a single band at ~59 kDa; calculated molecular mass, 64.5 kDa); in solution, the enzyme is a homodimer (~105 kDa; gel filtration). As isolated, CDH contains 0.8 ± 0.05 ThDP, 1.0 ± 0.02 Mg^{2+}, and 1.0 ± 0.015 flavin adenine dinucleotide (FAD) per monomer as a second organic cofactor, the role of which remains unclear. Strong reductants, Ti(III)-citrate, Na^+-dithionite, and the photochemical 5-deazaflavin/oxalate system, led to a partial reduction of the FAD chromophore. The cleavage product of CDO, 6-oxohexanoate, was also a substrate; the corresponding cyclic 1,3- and 1,4-diones did not react with CDH, nor did the *cis*- and *trans*-cyclohexane diols. The enzymes acetohydroxyacid synthase (AHAS) from *Saccharomyces cerevisiae*, pyruvate oxidase (POX) from *Lactobacillus plantarum*, benzoylformate decarboxylase from *Pseudomonas putida*, and pyruvate decarboxylase from *Zymomonas mobilis* were identified as the closest relatives of CDH by comparative amino acid sequence analysis, and a ThDP binding motif and a 2-fold Rossmann fold for FAD binding could be localized at the C-terminal end and central region of CDH, respectively. A first mechanism for the ring cleavage of CDO is presented, and it is suggested that the FAD cofactor in CDH is an evolutionary relict.

Alicyclic compounds, such as steroids and terpenes, are widespread in nature. They are produced by plant cells as secondary metabolites and occur in fossil fuels. Microorganisms can convert these compounds to cellular metabolites under oxic and anoxic conditions. Their biodegradation proceeds via C—C bond ring cleavage to form an aliphatic intermediate, which can be further degraded by β-oxidation. In aerobic bacteria, the cleavage of the cyclic compound is catalyzed by a NADPH-dependent, flavin-containing monooxygenase. For example, cyclohexanone is converted to ε-caprolactone in a Bayer-Villiger-type reaction (14). Subsequently, the lactone is hydrolyzed to 6-hydroxyhexanoate (63), followed by two NAD^+/$NADP^+$-dependent oxidation steps with adipate as the final product. In anaerobes, such as *Pseudomonas* sp. strain K601, cyclohexanone is oxidized via 2-cyclohexenone and 3-hydroxycyclohexanone to cyclohexane-1,3-dione, which then is transformed to 5-oxohexanoate (13). With the isolation of the denitrifying bacterium *Azoarcus* sp. strain 22Lin grown on cyclohexane-1,2-diol, a new degradation pathway for alicyclic compounds has been discovered (Fig. 1). The formation of 6-oxohexanoate from cyclohexane-1,2-dione and of adipate during NAD^+ reduction suggested that strain 22Lin had a carbon-carbon hydrolase that transformed cyclohexane-1,2-dione into 6-oxohexanoate (22).

Here, the purification and characterization of the ring-cleaving enzyme from denitrifying *Azoarcus* sp. strain 22Lin, termed cyclohexane-1,2-dione hydrolase (CDH) (EC 3.7.1.11), is described. CDH represents a novel member of the thiamine diphosphate (ThDP)-dependent enzyme family; it converts cyclohexane-1,2-dione (CDO) into 6-oxohexanoate, and it catalyzes its oxidation to adipate (Fig. 1). A similar hydrolytic cleavage of a cyclic compound, the conversion of 3*D*-(3,5/4)-trihydroxycyclohexane-1,2-dione to 5-deoxy-D-glucuronic acid, was described as part of the *myo*-inositol catabolism in *Bacillus subtilis* (65, 66). The enzyme encoded by *iolD* showed significant homology to the ThDP-dependent enzyme acetolactate

* Corresponding author. Mailing address: Fachbereich Biologie, Universitaet Konstanz, Universitaetsstrasse 10, 78457 Constance, Germany. Phone: 497531-88-2103. Fax: 497531-88-2966. E-mail: peter.kroneck@uni-konstanz.de.

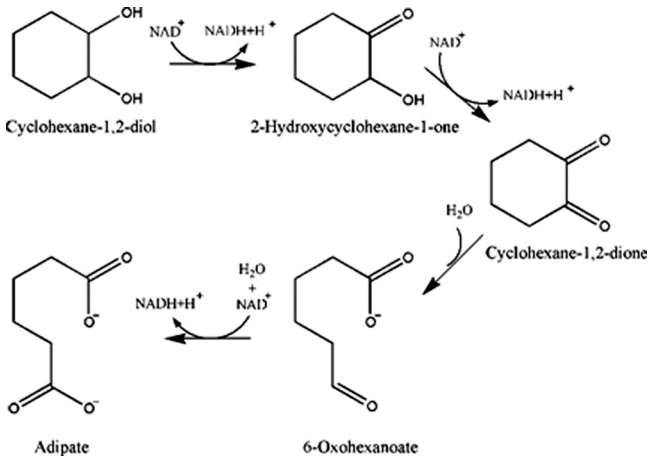

FIG. 1. Degradation of cyclohexane-1,2-diol by *Azoarcus* sp. strain 22Lin (22). The last two steps are catalyzed by cyclohexane-1,2-dione hydrolase (this work).

synthase from *Spirulina platensis* and *Synechococcus* sp. (26.4% and 26.0% identity for amino acids) (65). However, this enzyme has not yet been purified and characterized (K. Yoshida, personal communication). The conversion of the cyclic diketone CDO to 6-oxohexanoate proceeds via the cleavage of the C—C bond adjacent to a carbonyl group, a typical feature of catalysis by ThDP-dependent enzymes (31). In addition to ThDP and Mg^{2+}, CDH contains flavin adenine dinucleotide (FAD) as a second organic cofactor, which is proposed to be an evolutionary relict. The molecular and catalytic properties of CDH, including its amino acid sequence, are compared with those of representative ThDP and ThDP/FAD-dependent enzymes. Furthermore, a first mechanism for the transformation of CDO to 6-oxohexanoate is presented.

MATERIALS AND METHODS

Cultivation and preparation of cell fractions. *Azoarcus* sp. strain 22Lin (DSM 15408) was grown as described previously (22); cells were harvested in the late exponential growth phase and frozen at −70°C. Frozen cells (10 g [wet weight]) were thawed and suspended in 50 mM MES (morpholineethanesulfonic acid), pH 6.5, containing 1 mM $MgCl_2$, 0.5 mM ThDP, and a few crystals of DNase I. The cells were disrupted by three passages in a French press (130 MPa; Aminco). The crude extract was centrifuged at 100,000 × *g* (90 min; 4°C), the pellet was discarded, and the supernatant containing both periplasmic and cytoplasmic proteins (soluble fraction) was used for enzyme preparation.

Enzyme purification. All chromatographic steps were carried out at 4°C with a fast protein liquid chromatography (FPLC) system (GE Healthcare). The soluble fraction was applied to a DEAE Sepharose Fast Flow column equilibrated with 50 mM MES, pH 6.5, containing 1 mM $MgCl_2$ and 0.5 mM ThDP. CDH was eluted with a linear NaCl gradient (50 to 250 mM) at ~160 mM NaCl. Fractions containing CDH were combined, and NaCl was removed by ultrafiltration (cutoff, 30 kDa; Amicon) and subsequent dilution with MES buffer. The desalted solution was loaded onto a Resource Q30, and a linear NaCl gradient (0 to 300 mM) led to the elution of CDH at ~125 mM NaCl. Fractions containing CDH were combined, concentrated by ultrafiltration (30 kDa), and loaded onto a Superdex 200 HiLoad 26/60 gel filtration column equilibrated with MES, pH 6.5, containing 1 mM $MgCl_2$, 0.5 mM ThDP, and 150 mM NaCl. Pure CDH was frozen in liquid nitrogen and stored as concentrated aliquots (10 to 22 $mg \cdot ml^{-1}$) at −70°C or in liquid nitrogen.

Protein concentration. Protein was measured according to the method of Smith et al. (57), with bovine serum albumin as the standard; pure CDH was also measured spectrophotometrically at 434 nm (molar absorption coefficient at 434 nm [ε_{434}] = 6.81 $mM^{-1} \cdot cm^{-1}$ at pH 7.0).

Molecular mass. The molecular mass of native CDH was determined by analytical gel filtration with a Superdex 200 HiLoad 26/60 column equilibrated with 50 mM MES, pH 6.0; the column was calibrated against cytochrome *c* (12.4 kDa), carbonic anhydrase (29 kDa), conalbumin (76 kDa), alcohol dehydrogenase (150 kDa), and β-amylase (200 kDa) from Sigma. The molecular mass was calculated from the amino acid sequence and was determined by SDS/PAGE on a 12.5% polyacrylamide gel (33); the markers were lysozyme (14.4 kDa), trypsin inhibitor (21.5 kDa), carbonic anhydrase (31 kDa), ovalbumin (45 kDa), serum albumin (66.2 kDa), and phosphorylase *b* (97.4 kDa) (Bio-Rad). The gels were stained with Coomassie brilliant blue G250 (67) or silver (48).

Isoelectric point. The pI was determined by chromatofocusing; 3 mg of pure CDH, dissolved in 25 mM Bis-Tris buffer, pH 6.3, was loaded on a Mono P FPLC column equilibrated with the same buffer; 10-fold diluted Polybuffer 74 (GE Healthcare), pH 4.0, was the eluent.

Determination of flavin. Samples were analyzed by high-performance liquid chromatography (HPLC) (Sykam) with a Gromsil C_{18} reversed phase column that was tempered at 35°C and equilibrated with 20 mM NaP_i buffer, pH 6.0. FAD, flavin mononucleotide (FMN), and riboflavin were eluted by a linear gradient (0 to 43% methanol) and identified by comparison with appropriate standards. FAD was quantified after trichloroacetic acid (TCA) precipitation; the sample (120 μl) was incubated with 40 μl 70% (vol/vol) TCA on ice in the dark (5 min) and centrifuged at 12 000 × *g* (5 min), and the pH of the supernatant was adjusted to pH 7.0 by the addition of 0.5 M K_2HPO_4 and 2.0 M NaOH (8). Free FAD was determined at 450 nm (ε_{450} = 11.30 $mM^{-1} \cdot cm^{-1}$) (34, 64).

Determination of thiamine. Samples were oxidized with 0.6 mM $K_3[Fe(CN)_6]$ in 14.7% NaOH (ratio, 2.6:1) to the corresponding thiochromes, which have a characteristic fluoresence (λ_{ex} = 370 nm; λ_{em} = 444 nm [6]). They were analyzed on an HPLC system equipped with a diode array detector 400 and an SFM 25 fluorescence detector (Kontron Instruments), with a Gromsil C_{18} reversed phase column that had been equilibrated with 25 mM KP_i buffer, pH 8.4. Thiochrome, thiochrome monophosphate, and thiochrome diphosphate were eluted by a linear gradient (12 to 100% methanol) and identified by comparison to standards.

Metal analysis. Samples were transferred by dialysis to 10 mM or 5 mM MES/NaOH, pH 6.5, and were analyzed for Mg, Ca, and Mn by inductively coupled plasma mass spectrometry (ICP-MS) (Spurenanalytisches Laboratorium Dr. Baumann, Maxhuette-Haidhof, Germany).

Enzyme activity. CDH activity was measured both photometrically and by HPLC. Routinely, CDH activity was assayed via its NAD^+-dependent reaction at 365 nm (NADH; ε_{365} = 3.4 $mM^{-1} \cdot cm^{-1}$) (69). Assays (1.0 ml) were run at 37°C in 100 mM HEPES, pH 8.0, containing 1.0 mM NAD^+, 0.10 mM CDO, 0.5 mM ThDP, and 5.0 mM $MgSO_4$ unless otherwise indicated. Freshly thawed aliquots of 10 mM or 100 mM CDO (Merck; purity, >98%) in H_2O were used. After incubation at 37°C (5 min) and measurement of the background NAD^+ reduction, reactions were started by adding CDH (0.4 to 0.8 μM); 1 unit is defined as the amount of enzyme required to oxidize 1 μmol CDO · min^{-1} under the assay conditions. The enzyme concentration was chosen so that a linear formation of NADH could be observed over a time interval of 10 to 20 s. For assays in the pH range from 5.0 to 10.0, the universal buffer containing 100 mM Na^+ citrate, 100 mM HEPES, 100 mM *N*,*N*-bis(2-hydroxyethyl)glycine (BICINE), 100 mM *N*-cyclohexyl-2-aminoethanesulfonic acid (CHES), and 0.15 mM CDO was used. Activity assays with various concentrations of enzyme were performed with 0.06 to 2.5 μM CDH. Further activity tests comprised variation of the concentrations of ThDP, $MgSO_4$, NAD^+, and CDO. In parallel, CDO and the reaction products 6-oxohexanoate and adipate were identified and quantitated on an Aminex HPX-87H ion-exchange column (18). All CDH activities are reported as the average of three determinations (standard deviation, 10 to 15%). Under the experimental conditions, the CDH-catalyzed cleavage of CDO displayed Michaelis-Menten kinetics, and k_{cat}^{app} and K_M^{app} were obtained with ORIGIN Pro8 software, using the Hill equation, including substrate inhibition (20).

UV-visible light (Vis) spectra. Absorption spectra were recorded with a Cary 50 instrument (Varian) equipped with a cell holder (fitted with a thermostat) and with the HP 8452 A diode array spectrophotometer (Hewlett Packard).

Exclusion of dioxygen. Experiments in the absence of dioxygen were carried out in an anaerobe chamber (95% N_2, 5% H_2; Coy) equipped with a Palladium catalyzator type K-0242 (0.5% Pd/Al_2O_3; ChemPur). Dioxygen was removed from buffers and solutions by 8 to 10 cycles of degassing and flushing with argon 4.9 (Messer Griesheim) at a vacuum line (3). Traces of dioxygen were removed from the argon 4.9 via passage through a glass/copper system filled with BTS Catalyst R3-11 (BASF). Glassware, plasticware, and buffers were stored for at least 24 h in the chamber prior to use, in order to equilibrate with the N_2/H_2 atmosphere.

Oxidation-reduction experiments. Titrations under dioxygen exclusion were carried out in a double-septum Thunberg-type cell (1). The reactant was added

TABLE 1. Purification of CDH from *Azoarcus* sp. strain 22Lin

Purification[a]	Total protein (mg)	Total activity (U)[b]	Sp act (mU · mg^{-1})	Optical index (A_{280}/A_{434})	Purification factor	% Yield
Crude extract	1,157	ND[c]	ND	ND	ND	ND
Soluble fraction	607	61.9	102	16.1	1	100
DEAE-sepharose	95	36.1	380	14.8	3.8	58
Resource Q30	47	21.6	460	10.8	4.5	35
Superdex 200	24	16.25	677	10.7	6.6	26

[a] Ten grams of cells (wet weight).
[b] One unit is equal to 1 μmol CDO min^{-1}.
[c] ND, not done.

in steps of 2.5 to 20 μl with a gas-tight syringe (Hamilton). For the photochemical reduction of CDH by oxalate/K^+-5-deaza-isoalloxazine-3-propanesulfonate (39), the system was deaerated by degassing and flushing with argon.

Bacterial genomic DNA. Genomic DNA from *Azoarcus* sp. strain 22Lin was prepared according to the method of Maniatis et al. (38) with minor modifications. Frozen cells (~2 g) were suspended in 20 ml ATL-Lysis buffer (Qiagen) and incubated for 30 min at 50°C in a water bath under gentle agitation to homogenize the solution. After addition of 0.6 mg · ml^{-1} lysozyme, the mixture was incubated for 30 min at 42°C with occasional gentle stirring. Proteins were digested with 0.2 mg · ml^{-1} proteinase K (Gibco BRL) during 30 min of incubation at 45°C, with the solution mildly shaken every 10 min. After addition of 1% (wt/vol) SDS and 60 min of incubation at 45°C with gentle shaking every 20 min, the solution was centrifuged at 12,000 × *g* (10 min; 4°C) and filtered through paper to eliminate larger debris. To remove bacterial proteins, the supernatant was extracted with phenol. Half a volume of phenol equilibrated with Tris-EDTA (TE) buffer, pH 8.0, was added to the supernatant and thoroughly mixed for 10 min by gentle shaking. Then, half a volume of chloroform-isoamyl alcohol (24:1) was added, thoroughly mixed by gentle inversion for 3 min, and centrifuged (12,000 × *g*; 10 min; 4°C). The upper aqueous phase was subjected to a second phenol-chloroform extraction, followed by a final chloroform-isoamyl alcohol (24:1) extraction to remove remaining traces of phenol (centrifugation, 12,000 × *g*; 10 min; 4°C). Purified DNA was precipitated in the form of white filaments upon adding 1/10 volume of 3 M sodium acetate, pH 6.4, and 2 volumes of ethanol to the aqueous phase. DNA was collected with a glass rod and washed 3 times with 70% (vol/vol) ethanol; excess liquid was removed with clean cellulose, and the DNA was dissolved in 500 μl TE buffer.

Sequence analysis. The N-terminal sequence was done by Toplab, Gesellschaft für angewandte Biotechnologie mbH (Munich). The CDH sample was reacted with 1,4-dithiothreitol, alkylated with iodoacetamide, and cleaved with trypsin. The internal protein fragments were separated by capillary HPLC and analyzed by automated Edman degradation. Three tryptic peptide sequences were used to design several degenerate oligonucleotides (MWG Biotech). These were used in PCRs with genomic *Azoarcus* DNA as a template; PCR (27, 49) was carried out with RedTaq DNA Polymerase (Sigma) or the Expand Long Template PCR System (Roche Diagnostics) containing 1:50 *Pwo* DNA polymerase and RedTaq on a GeneAmp PCR System 9700 (PE Applied Biosciences). Typically, 0.4 μM forward primer, 0.4 μM reverse primer, 0.02 to 0.04 U · μl^{-1} RedTaq, 0.8 μM deoxynucleoside triphosphates (dNTPs), 2.5 μl 10× amplification buffer (Sigma), and 5 to 100 ng DNA were used for amplification in a total volume of 25 μl. PCR products were analyzed on a 1% agarose gel with subsequent ethidium bromide staining in the presence of the 1-kb ladder length standard (Gibco BRL) and purified with a QIAquick PCR Purification Kit (Qiagen) or a QIAquick Gel Extraction Kit (Qiagen) after excision from a preparative agarose gel. For the sequencing reactions, PCR products were amplified according to Applied Biosystems protocols, using fluorescence-marked dideoxynucleotide triphosphates in the ABI Prism BigDye Terminator Cycle Sequencing Ready Reaction Kit (Applied Biosystems). Typically, 10 ng PCR product, 10 pmol degenerated primer or 5 pmol specific primer, 1 μl Terminator Ready Reaction Mix (Applied Biosystems), and 1.5 μl 5× sequencing buffer (Applied Biosystems) were used in a total volume of 10 μl. After ethanol precipitation according to the Applied Biosystems manual (version 2.0), the purified product was analyzed on a 3100 Capillary Array with 16 capillaries and further examined with the program Sequence Navigator (Applied Biosystems).

Anchor-ligated genome walking. The anchor-ligated PCR approach in combination with nested PCR allows one to obtain the sequence of the unknown surrounding regions flanking a known DNA fragment. Here, the Universal GenomeWalker Kit (Clontech) was used with adapters 1 and 2 (adapter 1, 5′-CGA CTC ACT ATA GGG CAC GCG TGG TCG ACG GCC CGG GCT GGT-3′; adapter 2, 5′-ACC AGC CCG GG-3′) and adapter primers AP1 and AP2 (AP1, 5′-CGA CTC ACT ATA GGG CAC GC-3′; AP2, 5′-GGC ACG CGT GGT CGA CGG-3′). Adapter 2 contained an additional NH_2 group at its 3′ end to prevent elongation by the DNA polymerase.

RESULTS

Enzyme purification. Active CDH from *Azoarcus* was purified to homogeneity (SDS-PAGE) by a three-step chromatographic procedure. The activity of CDH was found exclusively in the soluble fraction and could be increased approximately 7-fold (Table 1). The yield of pure CDH enzyme from five different cultivations of *Azoarcus* sp. strain 22Lin amounted to 3.0 ± 0.5 mg/g (wet weight) cells; the specific activity of pure CDH was 825 ± 150 mU mg^{-1} (10 preparations; standard assay).

Molecular parameters and cofactors. CDH is an acidic protein, with a pI of 4.5. On SDS-PAGE, it gives a single band at ~59 kDa compared to the calculated mass of 64.5 kDa (the amino acid sequence plus FAD, ThDP, and Mg^{2+}). Gel filtration gives a molecular mass of ~105 kDa, indicating that the enzyme exists as a homodimer in solution.

CDH-containing fractions show an intense yellow color; the UV-Vis spectrum of the pure enzyme exhibits maxima at 371 nm and 434 nm, with shoulders at 357 nm, 412 nm, and 457 nm, typical of flavoproteins (Fig. 2). A yellow compound was released after denaturation of CDH with TCA, which was identified as FAD by HPLC analysis (data not shown). Its quantification (triplicate) gave 1.0 ± 0.015 noncovalently bound FAD per CDH monomer. The supernatant of TCA-treated CDH was analyzed for thiochrome derivatives. A thiochrome compound eluted after 6.46 min and was identified as thiochrome diphosphate. Quantitative analysis (triplicate) revealed 0.8 ± 0.05 ThDP per CDH monomer (purified in 50 mM MES, pH 6.5, 1 mM $MgCl_2$, 0.5 mM ThDP) compared to ~0.23 ThDP per monomer (purified in 50 mM Tris, pH 8.3, or 100 mM HEPES, pH 7.0). ICP-MS analysis gave 1.0 ± 0.02 Mg^{2+} per monomer. $Mn^{2+}$and Ca^{2+} were absent.

Enzyme activity with CDO as a substrate. The formation of 6-oxohexanoate from CDO and its subsequent oxidation to adipate by NAD^+ is catalyzed by CDH, as documented by HPLC (reference 18 and data not shown). The activity of CDH could be enhanced by increasing the concentration of CDH in the standard assay to 0.02 mg · ml^{-1}; higher concentrations caused saturation. The specific activity of CDH was highest at pH 8.0 in universal buffer (pH range, 5 to 10) containing 100

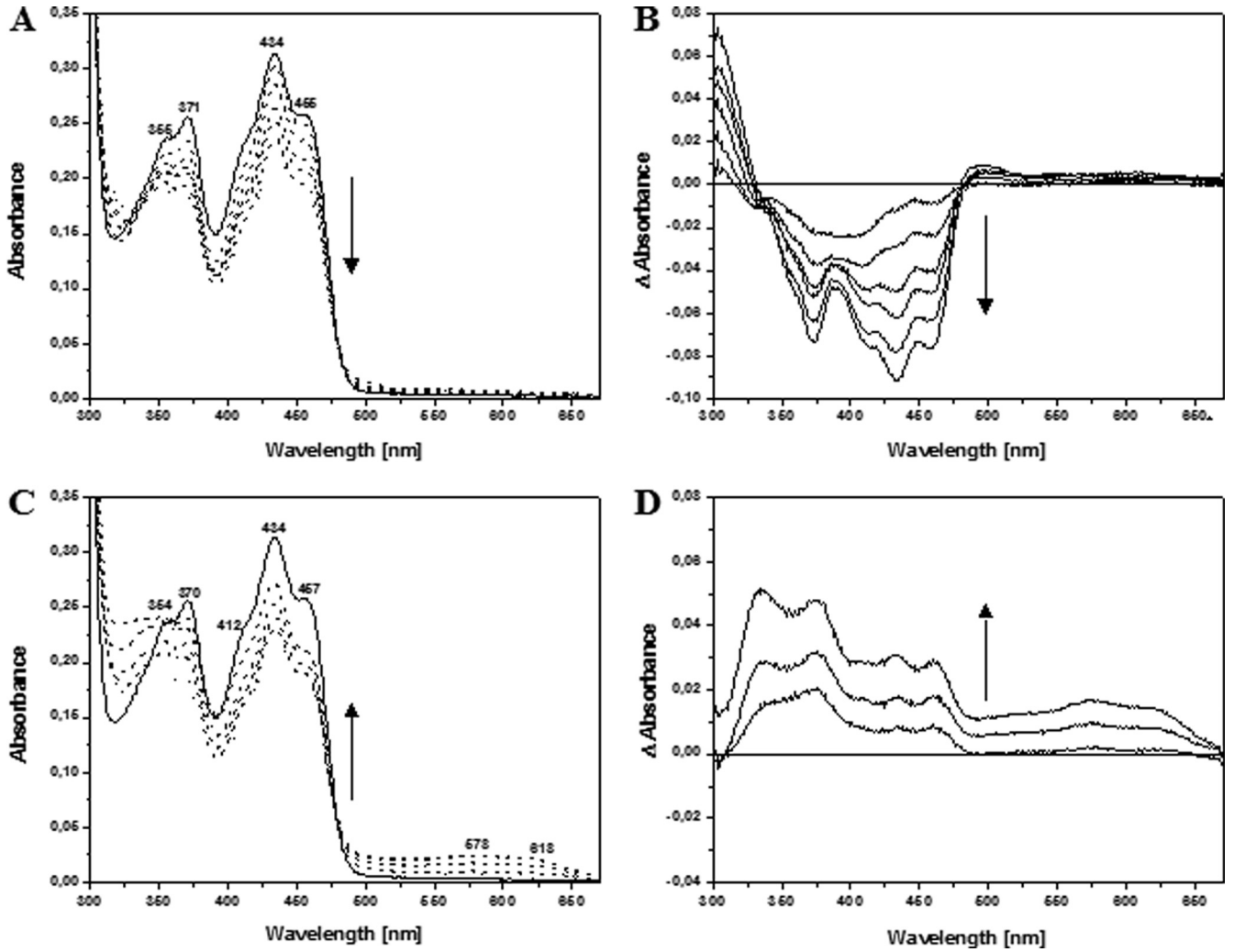

FIG. 2. UV-Vis spectra of the photochemical reduction of CDH (A and B) and reoxidation with $K_3[Fe(CN)_6]$ (C and D) (30 μM CDH, 20 mM Na^+ oxalate, 3 μM 5-deazaflavin in 50 mM HEPES, pH 8.0). (A) CDH as isolated (solid line) and after 30 s and 4, 12, 17, 22, and 30 min irradiation. (B) Difference spectra of photochemical reduction. (C) Partially reduced CDH (30 min irradiation) and after addition of 7 μM, 48 μM, and 91 μM $K_3[Fe(CN)_6]$; solid line, CDH fully oxidized as isolated. (D) Difference spectra of reoxidation. The arrows indicate spectral changes upon increase of the irradiation time (A and B) and upon addition of $K_3[Fe(CN)_6]$ (C and D).

mM Na^+ citrate, 100 mM HEPES, 100 mM BICINE, and 100 mM CHES (see Fig. S1 in the supplemental material). Note that the activity decreased significantly at this high ionic strength: 130 ± 15 versus 825 ± 150 mU mg^{-1} under standard assay conditions in 100 mM HEPES buffer, pH 8.0. Furthermore, the addition of sodium chloride to the assay mixture, e.g., 50 mM or 200 mM NaCl, reduced the specific activity of CDH by 30% and 70%, respectively (data not shown). At pH >8.0, the dissociation of the cofactor ThDP occurred, as reported for pyruvate decarboxylase (26, 46), leading to a decrease in activity.

The longer the reaction mixture with CDO was kept at 37°C, pH 8.0, before adding the enzyme, the higher was the resulting specific activity of CDH. In parallel, the concentration of the CDO monoenol decreased when followed at 260 nm, indicating the formation of the CDO monohydrate (2, 36) (Fig. 3). Typically, the activity increased to 113% ± 2% after incubation for 5 min versus 124% ± 2% for 10 min.

Variation of the concentrations of CDO and NAD^+ led to the data displayed in Fig. 4. Here, the substrate CDO began to inhibit the reaction at a concentration around 150 μM under the experimental conditions. The data followed Michaelis-Menten kinetics, with the following apparent parameters: $k_{cat}^{app} = 1.6 \pm 0.1\ s^{-1}$, $K_m^{app} = 13.3 \pm 0.1$ μM, and $k_{cat}^{app}/K_m^{app} = 1.2 \pm 0.1 \times 10^5\ s^{-1}\ M^{-1}$ for CDO. In the case of NAD^+, the following parameters were obtained: $k_{cat}^{app} = 1.5 \pm 0.1\ s^{-1}$, $K_m^{app} = 164 \pm 31$ μM, and $k_{cat}^{app}/K_m^{app} = 0.91 \times 10^4\ s^{-1}\ M^{-1}$.

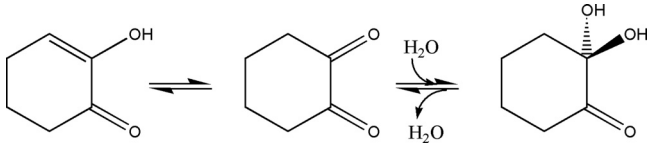

FIG. 3. Forms of cyclohexane-1,2-dione in aqueous solution (2, 36).

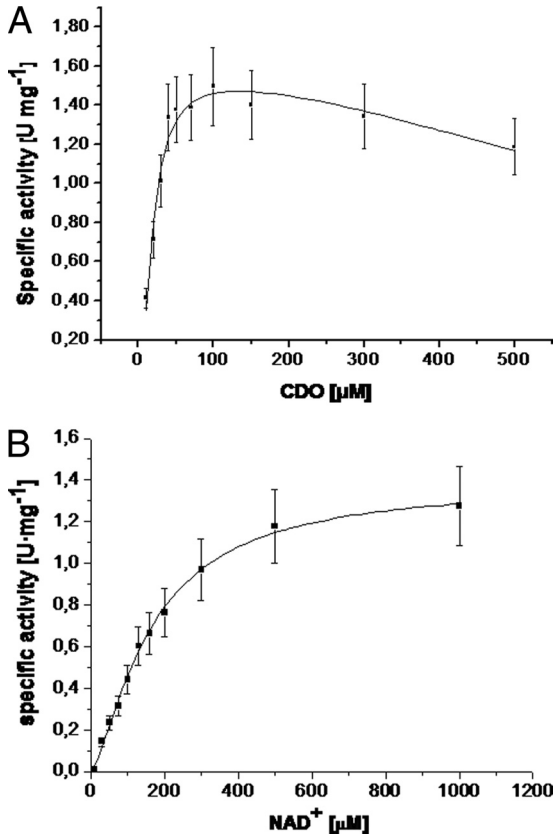

FIG. 4. (A) Dependence of the specific activity of CDH on the concentration of CDO (0.28 μM CDH, 0.5 mM ThDP, 5.0 mM $MgSO_4$, 1.0 mM NAD^+, 10 to 500 μM CDO, 0.10 M HEPES, pH 8.0; 37°C; 5 min substrate incubation at 37°C; fit as described in Materials and Methods). (B) Dependence of the specific activity of CDH on the concentration of NAD^+ (0.47 μM CDH, 0.5 mM ThDP, 5.0 mM $MgSO_4$, 10 to 1,000 μM NAD^+, 0.10 M HEPES, pH 8,0; 37°C; 5 min substrate incubation at 37°C; fit as described in Materials and Methods). The error bars indicate standard deviations.

Alternative substrates. So far, the only substrate of CDH studied in more detail was CDO. Its cleavage product, 6-oxohexanoate, is also a substrate of CDH and is converted to adipate by CDH in the presence of NAD^+, as shown by HPLC. The corresponding cyclic 1,3- and 1,4-diones did not react with CDH, nor did the *cis*- and *trans*-cyclohexane diols and the linear compounds 2-oxopentanoate and hexane-3,4-diketone (18). Pyruvate, a common substrate of many ThDP enzymes, such as acetolactate synthase (ALS), acetohydroxyacid synthase (AHAS), pyruvate oxidase (POX), or pyruvate decarboxylase, was not converted by CDH from *Azoarcus* sp. 22Lin (followed by HPLC and formation of NADH) as reported for these enzymes (12, 31, 62).

Oxidation-reduction experiments. Attempts to reduce the FAD cofactor of CDH in the absence of dioxygen yielded only partially reduced FAD with the reductants Ti(III)-citrate and Na^+-dithionite; L-ascorbate, NADH, $NaBH_4$, and CDO did not lead to any reduction of the FAD moiety. Maximum reduction of FAD was achieved photochemically with the oxalate/K^+-5-deaza-10-methyl-3-sulfopropyl-isoalloxazine system (39); however, irradiation intervals of up to 30 min were required. Reoxidation of photochemically reduced CDH with aliquots of $K_3[Fe(CN)_6]$ proceeded via the formation of the blue neutral flavin radical with its typical absorbance at 575 nm to 625 nm (Fig. 2). The concentration of the semiquinone amounted to 6.2 μM (~20% of total FAD) based on the extinction coefficient $\varepsilon_{580\text{-}620}$ (~4.00 $mM^{-1} \cdot cm^{-1}$) (37). The starting spectrum of the enzyme as isolated could not be fully restored (~85%), even after the addition of an excess of $K_3[Fe(CN)_6]$ (4 to 10 equivalents per CDH monomer), most likely because of radiation damage to the FAD chromophore.

Amino acid sequence and binding motifs. The N-terminal sequence of CDH (19 amino acids) and two further internal sequences (17 amino acids) constituted the starting point for primer design and the subsequent amplification of genomic DNA by PCR. The flanking regions of known DNA fragments were sequenced with the Anchor "ligated-genome-walking" approach. The nucleotide sequence of the CDH gene was determined for both strands to minimize potential sequencing errors. A Shine-Dalgarno sequence (5′-AGGAGA-3′ [consensus, 5′-AGGAGG-3′]) was located 6 nucleotides upstream of the initiation codon, ATG. It increases the efficiency of translation of the corresponding mRNA. Neither a −35 promoter region nor a Pribnow box was found directly upstream of the CDH gene. Stem-loop structures, often associated with the ends of transcripts, were found downstream of the CDH gene (data not shown). Additionally, the 300 nucleotides downstream of the CDH gene did not encode any longer open reading frame. This leads to the possibility that the CDH gene is part of an operon that ends behind it. The alignment of the amino acid sequence of CDH with representatives of the ThDP enzyme family that have known structures revealed the presence of three well-conserved regions, an N-terminal domain from amino acids (aa) 1 to 172, a central domain from aa 192 to 333, and a C-terminal domain from aa 350 to 545 (Fig. 5). The overall amino acid sequence identity between CDH and these enzymes is 24% to 28%. In all these sequences, the ThDP binding motif is located toward the C-terminal end. It starts with the highly conserved sequence GDG and ends with NN. In the CDH amino acid sequence, one of the two polar asparagines was replaced by threonine. The approximately 30 residues between GDG and NN are not highly conserved but exhibit several common features (25) that are also present in the CDH sequence. For example, 9 residues after the GDG sequence there is usually a negatively charged residue and, 10 residues further, a strictly conserved proline followed by two highly conserved valine and isoleucine residues. Between the proline and the NN sequence there is a cluster of 6 mainly hydrophobic side chains starting with V and I. Additionally, all the depicted sequences share the N-terminal glutamate (Fig. 5, red shading), which is supposed to be responsible for the formation of the ThDP-ylide and for the activation of ThDP (30, 42).

The central domain of CDH exhibits a 2-fold Rossmann fold, presumably for FAD binding, similar to the double Rossmann fold in POX (Fig. 5, green shading) (40). A potential conserved sequence motif for the POX FAD family fold was published by Dym and Eisenberg (16) and is marked by green arrowheads in Fig. 5. At these positions, CDH and AHAS show about 50% identity and 50% amino acids with similar physical and chemical properties (Fig. 5). In contrast, there are

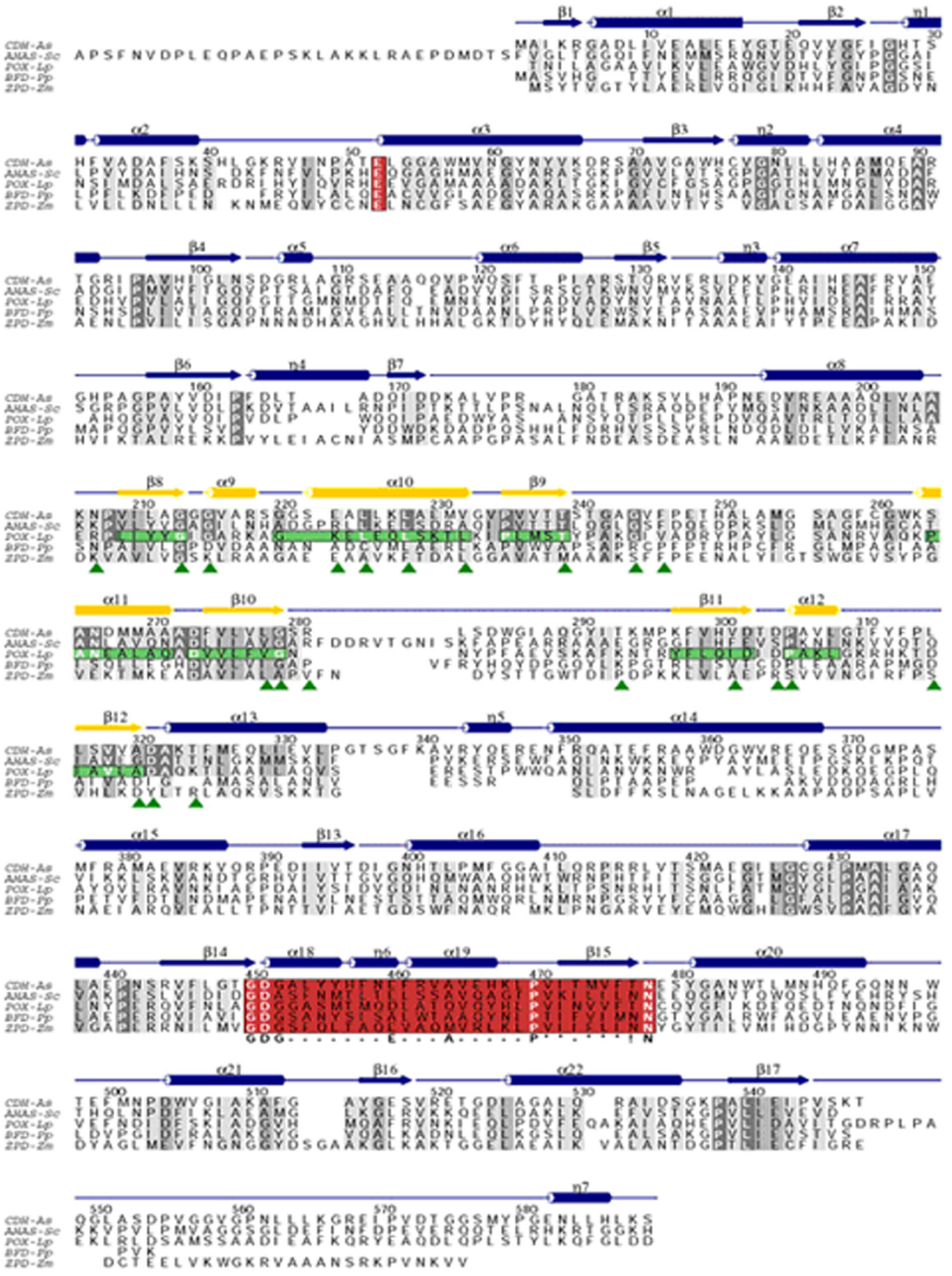

FIG. 5. Multiple amino acid sequence alignment of ThDP-dependent enzymes. CDH-As, cyclohexane-1,2-dione hydrolase from *Azoarcus* sp. 22Lin; AHAS-Sc, AHAS from *S. cerevisiae* (PDB code 1N0H); POX-Lp, POX from *L. plantarum* (1POW); BFD-Pp, benzoylformate decarboxylase from *P. putida* (1BFD); and ZPD-Zm, pyruvate decarboxylase from *Z. mobilis* (1ZPD). The highly conserved N-terminal glutamate and the ThDP binding motif are shaded in red. The green shading indicates the residues of POX-Lp building up β1, α1, β2, and α2 and β3, β4, α3, and β5 of the double Rossmann fold. The residues involved in the potential FAD conserved consensus motif (16) are marked with green arrowheads.

fewer conserved amino acids with benzoylformate decarboxylase and pyruvate decarboxylase, which do not contain FAD as a cofactor.

DISCUSSION

Molecular properties. When grown on cyclohexane-1,2-diol, denitrifying *Azoarcus* sp. strain 22Lin expressed cyclohexane-1,2-dione hydrolase, a novel member of the ThDP enzyme family. CDH cleaved the alicyclic compound CDO to the semialdehyde 6-oxohexanoate, followed by its oxidation to adipate (Fig. 1) (22). In solution, CDH appeared as a homodimer (gel filtration); the recently solved crystal structure of CDH (resolution, 1.26 Å), however, revealed a tetrameric protein architecture consisting of a dimer of dimers. Significant amounts of trimeric or tetrameric oligomers were not observed by gel filtration, dynamic light scattering, or analytic ultracentrifugation at higher concentrations of enzyme, including the conditions of crystallization (17; A. K. Steinbach et al., submitted for publication). Most ThDP-dependent enzymes are arranged as homotetramers, such as POX from *Lactobacillus plantarum* (56), benzoylformate decarboxylase from *Pseudomonas putida* (23), indolepyruvate decarboxylase from *Enterobacter cloacae* (54), or pyruvate decarboxylase from *Zymomonas mobilis* (41). Bacterial AHAS reveals a common $\alpha_2\beta_2$ tetrameric structure (21, 51), whereas AHAS from *Arabidopsis thaliana* (9) and transketolase from *Saccharomyces cerevisiae* (59) represent examples of dimeric ThDP enzymes. The only case where a ThDP-dependent enzyme has been reported to have a trimeric subunit composition under native conditions is the phosphonopyruvate decarboxylase from *Bacteroides fragilis* (68).

Cofactors. The ThDP cofactor was less tightly associated with the protein than FAD, and thus, ThDP and $MgCl_2$ had to be added during purification of CDH. $MgCl_2$ could be exchanged for $MgSO_4$; the enzyme was active but less stable against freezing and thawing. In contrast, FAD could be removed only under denaturing conditions. Exceptionally tight binding of both FAD and ThDP to the protein scaffold had been reported for POX from *L. plantarum* (56). From the crystal structures of several ThDP-dependent enzymes it is known that ThDP is located at the interface between the subunits, with the pyrophosphate group and the aminopyrimidine moiety attached to different subunits (15, 24, 35, 40, 44, 55). Consequently, dimers form as the minimum functional units of ThDP enzymes (50). In this way, ThDP plays a crucial role as a linker between neighboring subunits in the formation of the overall architecture of the enzyme. Moreover, quaternary structures of ThDP enzymes are often very sensitive to pH (32), ionic strength, and anions, such as chloride, sulfate, or phosphate (50, 54).

In general, flavoenzymes are involved in redox catalysis, with the isoalloxazine ring undergoing reversible oxidoreduction in one two-electron or two single-electron transfer steps (19). The FAD cofactor of CDH was unexpectedly difficult to reduce; the photochemical deazaflavin system (redox potential at pH 7.0 [$E^{0\prime}$] = −650 mV [5]) worked best, with ~45% reduction of FAD at pH 8.0 (Fig. 2). Similar behavior has been reported for the ThDP-dependent flavoenzyme glyoxylate carboligase from *Escherichia coli*, which catalyzes the condensation of two molecules of glyoxylate to tartronic semialdehyde, a nonredox reaction (11, 29). ALS and AHAS constitute another set of unusual flavoenzymes in this respect (43, 53). However, the enzyme-bound FAD in AHAS can be reduced during catalysis in a side reaction; transient flavin radicals have not been observed in this case (61). Independent of the redox state of FAD, the rate of the physiological condensation reaction is essentially the same in ALS, although the latter shows an absolute requirement for FAD (52). Aside from CDH, glyoxylate carboligase, ALS, and AHAS, only a few other flavoenzymes, such as oxynitrilase, have been described that will not catalyze a net redox reaction despite an absolute requirement for FAD (7, 28).

Enzyme activity. With CDO as a substrate, the activity of CDH was highest at pH 8.0 (see Fig. S1 in the supplemental material), whereas lower pH values were reported for POX from *L. plantarum* (pH 5.7) (60) and various 2-ketoacid decarboxylases (20, 41). CDH showed a relatively steep increase in specific activity in the pH range from 6.5 to 8.0, which might be related to the formation of the CDO monohydrate. The keto-enol transformation of CDO (Fig. 3) is slow in aqueous solution but is catalyzed by both acids and bases. As pointed out by Bakule and Long (2, 36), the ketone is almost entirely present in aqueous solution as its monohydrate, which forms rapidly. In line with this finding, the ketone, and not the enol form of indolepyruvate, was shown to be the active substrate of indolepyruvate decarboxylase (54, 58). The observed decrease in activity upon addition of NaCl was due to the binding of the chloride anion in close proximity to the ThDP cofactor in CDH (17; Steinbach et al., submitted).

The kinetic parameters of CDH with CDO as a substrate (K_m^{app} = 13.3 μM and $k_{cat}^{app}/K_m^{app} = 1.2 \times 10^5\ s^{-1}\ M^{-1}$) are in the range reported for indolepyruvate decarboxylase/indolepyruvate from *Enterobacter cloacae* (K_m = 20 μM and $k_{cat}/K_m = 2 \times 10^5\ s^{-1}\ M^{-1}$) and phosphonopyruvate decarboxylase/phosphonopyruvate from *Bacteroides fragilis* (K_m = 3.2 μM and $k_{cat}/K_m = 3.2 \times 10^6\ s^{-1}\ M^{-1}$) (54, 68). Recently, the catalytic properties of several ThDP-dependent 2-ketoacid decarboxylases have been compared. With pyruvate as a substrate, the bacterial enzymes exhibited similar kinetic parameters, with K_m values in the range from 1.3 to 2.8 mM (20). Notably, CDH did not accept pyruvate as a substrate, and it did not react with compounds structurally related to either CDO or 6-oxohexanoate (18).

Amino acid sequence and relation to known ThDP enzymes. The multiple amino acid sequence alignment of CDH, yeast AHAS, *L. plantarum* POX, *P. putida* benzoylformate decarboxylase, and *Zymomonas mobilis* pyruvate decarboxylase documented that these five proteins share similarities over their entire sequence lengths and that they have evolved from a common ancestor (Fig. 5). A remarkable extent of similarity was found in a single region of 51 amino acids that encompassed the ThDP binding sites of all five enzymes. A second region with significant identity was present in their central domains (135 to 140 amino acids) that included the double Rossmann fold for FAD binding. This explains the higher homology of CDH, AHAS, and POX in this region compared to benzoylformate decarboxylase and pyruvate decarboxylase. The last two enzymes do not possess the FAD cofactor. According to Chang and Cronan (10), the acetate-producing POX was the ancestor of the enzymes ALS and AHAS rather

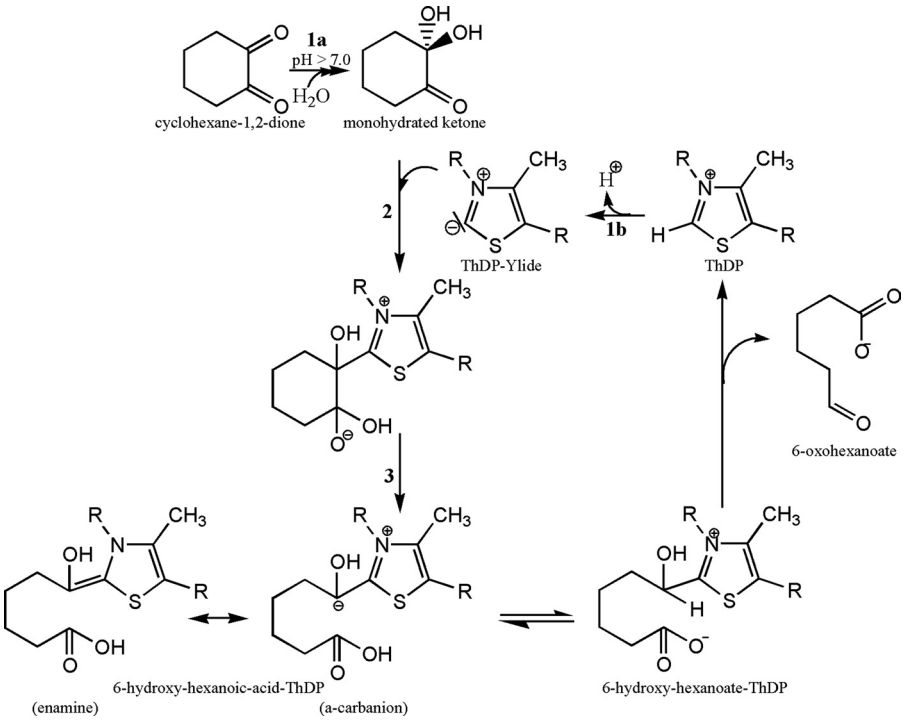

FIG. 6. Reaction mechanism for the C—C bond ring cleavage of CDO catalyzed by CDH (17), in accordance with the reaction mechanism of POX from *L. plantarum* (60).

than the reverse situation. They proposed that the flavin required for AHAS activity had only a structural role, that of facilitating protein-protein interactions. They argued by the rule of parsimony that flavins would not have first evolved to perform a structural role in protein folding. For the vast majority of proteins, and even in the case of FAD-independent ALS (45), this role has been fulfilled by amino acid side chain interactions. The need for FAD in maintaining structural integrity was also found for the acetate-producing POX (4). Identical cofactor requirements, similar catalytic properties, and high homology in amino acid sequence alignment support the assumption that CDH is closely related to ALS and AHAS. Thus, CDH also could have originated from POX, or another common redox enzyme ancestor, with FAD being an evolutionary relict.

Mechanism of the C—C bond ring cleavage. Following the ideas developed for several ThDP-dependent enzymes, including POX (31, 42, 60, 62), a first mechanism for the cleavage of CDO to 6-oxohexanoate was proposed, with the ThDP-ylide undergoing a nucleophilic attack on the carbonyl group of the cyclic ketone CDO, which is predominantly present as monohydrate in solution (Fig. 6) (17). The subsequent C—C bond ring cleavage yields the α-carbanion, followed by protonation to give the 6-hydroxyhexanoate-ThDP adduct. The mechanism of the subsequent NAD^+-dependent oxidation of the semialdehyde 6-oxohexanoate to adipate (Fig. 1) remains unclear at this point, as the redox-active cofactor FAD seems not to participate in catalysis. Although the present experimental data tend to support a direct hydride transfer from 6-oxohexanoate to NAD^+ and not an electron transfer via the FAD moiety as reported for AHAS (61), no obvious binding site for NAD^+ could be identified in the amino acid sequence or in the crystal structure of CDH (Steinbach et al., submitted).

Outlook. ThDP-dependent enzymes are versatile catalysts and open a wide field for engineering novel substrate specificities and reactivities that are of biotechnological interest (47). Although CDH is related to other members of the ThDP enzyme family with regard to its molecular architecture and mode of action, the enzyme is special: it is the first ThDP-dependent enzyme that cleaves an aliphatic ring, thereby enlarging the substrate spectrum of this enzyme family. CDH is also quite remarkable, as it catalyzes a NAD^+-dependent oxidation without employing the FAD cofactor adjacent to the ThDP active center in redox catalysis.

ACKNOWLEDGMENTS

We thank Christina Probian (MPI Bremen) for the cultivation of *Azoarcus*, Thomas Lohmiller (Universitaet Konstanz) for the generous gift of 6-oxohexanoate, and Sandro Ghisla (Universitaet Konstanz) for helpful discussions.

Financial support by the Deutsche Forschungsgemeinschaft (to P.M.H.K. and U.E.) and the Max-Planck-Gesellschaft (to J.H. and U.E.) is gratefully acknowledged.

REFERENCES

1. **Averill, B. A., J. R. Bale, and W. H. Orme-Johnson.** 1978. Displacement of iron-sulfur clusters from ferredoxins and other iron-sulfur proteins. J. Am. Chem. Soc. **100:**3034–3043.
2. **Bakule, R., and F. A. Long.** 1963. Keto-enol transformation of 1,2-cyclohexanedione. I. Hydration and keto-enol equilibria. J. Am. Chem. Soc. **85:**2309–2312.
3. **Beinert, H., W. H. Orme-Johnson, and G. Palmer.** 1978. Special techniques for the preparation of samples for low-temperature EPR spectroscopy. Methods Enzymol. **54:**111–132.
4. **Bertagnolli, B. L., and L. P. Hager.** 1993. Role of flavin in acetoin production by two bacterial pyruvate oxidases. Arch. Biochem. Biophys. **300:**364–371.

5. **Blankenhorn, G.** 1976. Nicotinamide-dependent one-electron and two-electron (flavin) oxidoreduction: thermodynamics, kinetics, and mechanism. Eur. J. Biochem. **67:**67–80.
6. **Bontemps, J., et al.** 1984. Determination of thiamine and thiamine phosphates in excitable tissues as thiochrome derivatives by reversed-phase high-performance liquid chromatography on octadecyl silica. J. Chromatogr. **307:** 283–294.
7. **Bornemann, S.** 2002. Flavoenzymes that catalyse reactions with no net redox change. Nat. Prod. Rep. **19:**761–772.
8. **Buechert, T.** 1997. Untersuchungen zur Struktur und Funktion des Eisen-Schwefel-Flavoenzyms Adenosin-5′-Phosphosulfat Reduktase aus *Desulfovibrio desulfuricans* (Essex). Ph.D. thesis, Universitaet Konstanz, Konstanz, Germany.
9. **Chang, A. K., and R. G. Duggleby.** 1997. Expression, purification and characterization of *Arabidopsis thaliana* acetohydroxy acid synthase. Biochem. J. **327:**161–169.
10. **Chang, Y.-Y., and J. E. Cronan, Jr.** 1988. Common ancestry of *Escherichia coli* pyruvate oxidase and the acetohydroxy acid synthases of the branched-chain amino acid biosynthetic pathway. J. Bacteriol. **170:**3937–3945.
11. **Chang, Y.-Y., A.-Y. Wang, and J. E. Cronan, Jr.** 1993. Molecular cloning, DNA sequencing, and biochemical analyses of *Escherichia coli* glyoxylate carboligase. An enzyme of the acetohydroxy acid synthase-pyruvate oxidase family. J. Biol. Chem. **268:**3911–3919.
12. **Chipman, D., Z. Barak, and J. V. Schloss.** 1998. Biosynthesis of 2-aceto-2-hydroxy acids: acetolactate synthases and acetohydroxy acid synthases. Biochim. Biophys. Acta **1385:**401–419.
13. **Dangel, W., A. Tschech, and G. Fuchs.** 1989. Enzyme reactions involved in anaerobic cyclohexanol metabolism by a denitrifying Pseudomonas species. Arch. Microbiol. **152:**271–279.
14. **Donoghue, N. A., D. B. Norris, and P. W. Trudgill.** 1976. The purification and properties of cyclohexanone oxygenase from *Nocardia globerula* CL1 and *Acinetobacter* NCIB 9871. Eur. J. Biochem. **63:**175–192.
15. **Dyda, F., et al.** 1993. Catalytic centers in the thiamin diphosphate dependent enzyme pyruvate decarboxylase at 2.4-ANG resolution. Biochemistry **32:** 6165–6170.
16. **Dym, O., and D. Eisenberg.** 2001. Sequence-structure analysis of FAD-containing proteins. Protein Sci. **10:**1712–1728.
17. **Fraas, S., et al.** 2009. Cyclohexane-1,2-dione hydrolase: a new tool to degrade alicyclic compounds. J. Mol. Catal. B Enzymatic **61:**47–49.
18. **Fraas, S.** 2009. Structural and functional studies on the FAD- and thiamindiphosphate-dependent cyclohexane-1,2-dione hydrolase from *Azoarcus* sp. strain 22Lin—the first α-ketolase. Ph.D. thesis. Universitaet Konstanz, Konstanz, Germany.
19. **Ghisla, S., and V. Massey.** 1989. Mechanisms of flavoprotein-catalyzed reactions. Eur. J. Biochem. **181:**1–17.
20. **Gocke, D., et al.** 2009. Comparative characterisation of thiamin diphosphate-dependent decarboxylases. J. Mol. Catal. B Enzymatic **61:**30–35.
21. **Grimminger, H., and H. E. Umbarger.** 1979. Acetohydroxy acid synthase I of *Escherichia coli*: purification and properties. J. Bacteriol. **137:**846–853.
22. **Harder, J.** 1997. Anaerobic degradation of cyclohexane-1,2-diol by a new *Azoarcus* species. Arch. Microbiol. **168:**199–204.
23. **Hasson, M. S., et al.** 1995. Purification and crystallization of benzoylformate decarboxylase. Protein Sci. **4:**955–959.
24. **Hasson, M. S., et al.** 1998. The crystal structure of benzoylformate decarboxylase at 1.6 Å resolution: diversity of catalytic residues in thiamin diphosphate-dependent enzymes. Biochemistry **37:**9918–9930.
25. **Hawkins, C. F., A. Borges, and R. N. Perham.** 1989. A common structural motif in thiamin pyrophosphate-binding enzymes. FEBS Lett. **255:** 77–82.
26. **Hübner, G., S. Koenig, and K. D. Schnackerz.** 1992. Correlation of cofactor binding and the quaternary structure of pyruvate decarboxylase as revealed by ^{31}P NMR spectroscopy. FEBS Lett. **314:**101–103.
27. **Innis, M. A., K. B. Myambo, D. H. Gelfand, and M. A. D. Brow.** 1988. DNA sequencing with *Thermus aquaticus* DNA polymerase and direct sequencing of polymerase chain reaction-amplified DNA. Proc. Natl. Acad. Sci. U. S. A. **85:**9436–9440.
28. **Jorns, M. S.** 1979. Mechanism of catalysis by the flavoenzyme oxynitrilase. J. Biol. Chem. **254:**12145–12152.
29. **Kaplun, A., et al.** 2008. Glyoxylate carboligase lacks the canonical active site glutamate of thiamine-dependent enzymes. Nat. Chem. Biol. **4:**113–118.
30. **Kern, D., et al.** 1997. How thiamine diphosphate is activated in enzymes. Science **275:**67–70.
31. **Kluger, R., and K. Tittmann.** 2008. Thiamin diphosphate catalysis: enzymic and nonenzymic covalent intermediates. Chem. Rev. **108:**1797–1833.
32. **König, S., D. Svergun, M. H. Koch, G. Huebner, and A. Schellenberger.** 1992. Synchrotron radiation solution X-ray scattering study of the pH dependence of the quaternary structure of yeast pyruvate decarboxylase. Biochemistry **31:**8726–8731.
33. **Laemmli, U. K.** 1970. Cleavage of structural proteins during the assembly of the head of bacteriophage T4. Nature **227:**680–685.
34. **Lampreia, J., et al.** 1990. The active centers of adenylylsulfate reductase from *Desulfovibrio gigas*. Characterization and spectroscopic studies. Eur. J. Biochem. **188:**653–664.
35. **Lindqvist, Y., G. Schneider, U. Ermler, and M. Sundstroem.** 1992. Three-dimensional structure of transketolase, a thiamine diphosphate dependent enzyme, at 2.5 Å resolution. EMBO J. **11:**2373–2379.
36. **Long, F. A., and R. Bakule.** 1963. Keto-enol transformation of 1,2-cyclohexanedione. II. Acid catalysis in strongly acidic media. J. Am. Chem. Soc. **85:**2313–2318.
37. **Macheroux, P.** 1999. UV-visible spectroscopy as a tool to study flavoproteins. Methods Mol. Biol. **131:**1–7.
38. **Maniatis, T., E. F. Fritsch, and J. Sambrook.** 1987. Molecular cloning: a laboratory manual. Cold Spring Harbor Laboratory Press, Cold Spring Harbor, NY.
39. **Massey, V., and P. Hemmerich.** 1977. A photochemical procedure for reduction of oxidation-reduction proteins employing deazariboflavin as catalyst. J. Biol. Chem. **252:**5612–5614.
40. **Muller, Y. A., G. Schumacher, R. Rudolph, and G. E. Schulz.** 1994. The refined structures of a stabilized mutant and of wild-type pyruvate oxidase from *Lactobacillus plantarum*. J. Mol. Biol. **237:**315–335.
41. **Neale, A. D., R. K. Scopes, R. E. Wettenhall, and N. J. Hoogenraad.** 1987. Pyruvate decarboxylase of *Zymomonas mobilis*: isolation, properties, and genetic expression in *Escherichia coli*. J. Bacteriol. **169:**1024–1028.
42. **Nemeria, N. S., S. Chakraborty, A. Balakrishnan, and F. Jordan.** 2009. Reaction mechanisms of thiamine diphosphate enzymes: defining states of ionization and tautomerization of the cofactor at individual steps. FEBS J. **276:**2432–2446.
43. **Pang, S. S., and R. G. Duggleby.** 1999. Expression, purification, characterization, and reconstitution of the large and small subunits of yeast acetohydroxy acid synthase. Biochemistry **38:**5222–5231.
44. **Pang, S. S., R. G. Duggleby, and L. W. Guddat.** 2002. Crystal structure of yeast acetohydroxy acid synthase: a target for herbicidal inhibitors. J. Mol. Biol. **317:**249–262.
45. **Pang, S. S., R. G. Duggleby, R. L. Schowen, and L. W. Guddat.** 2004. The crystal structures of *Klebsiella pneumoniae* acetolactate synthase with enzyme-bound cofactor and with an unusual intermediate. J. Biol. Chem. **279:**2242–2253.
46. **Pohl, M., K. Mesch, A. Rodenbrock, and M. R. Kula.** 1995. Stability investigations on the pyruvate decarboxylase from *Zymomonas mobilis*. Biotechnol. Appl. Biochem. **22:**95–105.
47. **Pohl, M., G. A. Sprenger, and M. Müller.** 2004. A new perspective on thiamine catalysis. Curr. Opin. Biotechnol. **15:**335–342.
48. **Rabilloud, T.** 1990. Mechanisms of protein silver staining in polyacrylamide gels: a 10-year synthesis. Electrophoresis **11:**785–794.
49. **Saiki, R. K., et al.** 1988. Primer-directed enzymatic amplification of DNA with a thermostable DNA polymerase. Science **239:**487–491.
50. **Schellenberger, A.** 1998. Sixty years of thiamin diphosphate biochemistry. Biochim. Biophys. Acta **1385:**177–186.
51. **Schloss, J. V., D. E. Van Dyk, J. F. Vasta, and R. M. Kutny.** 1985. Purification and properties of *Salmonella typhimurium* acetolactate synthase isozyme II from *Escherichia coli* HB101/pDU9. Biochemistry **24:**4952–4959.
52. **Schloss, J. V., L. Ciskanik, E. F. Pai, and C. Thorpe.** 1991. Acetolactate synthase: a deviant flavoprotein, p. 907–910. *In* B. Curti, S. Ronchi, and G. Zanetti (ed.), Flavins and flavoproteins: proceedings of the Tenth International Symposium on Flavins and Flavoproteins, Como, Italy, July 15-20, 1990. Walter de Gruyter, Berlin, Germany.
53. **Schloss, J. V.** 1992. Acetolactate synthase, p. 532–542. *In* F. Müller (ed.), Chemistry and biochemistry of flavoenzymes, vol. 3. CRC Press, Boca Raton, FL.
54. **Schütz, A., et al.** 2003. Studies on structure-function relationships of indolepyruvate decarboxylase from *Enterobacter cloacae*, a key enzyme of the indole acetic acid pathway. Eur. J. Biochem. **270:**2322–2331.
55. **Schütz, A., et al.** 2003. Crystal structure of thiamindiphosphate-dependent indolepyruvate decarboxylase from *Enterobacter cloacae*, an enzyme involved in the biosynthesis of the plant hormone indole-3-acetic acid. Eur. J. Biochem. **270:**2312–2321.
56. **Sedewitz, B., K. H. Schleifer, and F. Goetz.** 1984. Purification and biochemical characterization of pyruvate oxidase from *Lactobacillus plantarum*. J. Bacteriol. **160:**273–278.
57. **Smith, P. K., et al.** 1985. Measurement of protein using bicinchoninic acid. Anal. Biochem. **150:**76–85.
58. **Stowe, B. B.** 1955. The production of indoleacetic acid by bacteria. Biochem. J. **61:**9–10.
59. **Sundström, M., Y. Lindqvist, G. Schneider, U. Hellman, and H. Ronne.** 1993. Yeast *TKL1* gene encodes a transketolase that is required for efficient glycolysis and biosynthesis of aromatic amino acids. J. Biol. Chem. **268:**24346–24352.
60. **Tittmann, K., R. Golbik, S. Ghisla, and G. Huebner.** 2000. Mechanism of elementary steps of pyruvate oxidase from *Lactobacillus plantarum*. Biochemistry **39:**10747–10754.
61. **Tittmann, K., et al.** 2004. Electron transfer in acetohydroxy acid synthase as a side reaction of catalysis. Implications for the reactivity and partitioning of the carbanion/enamine form of (α-hydroxyethyl)thiamin diphosphate in a "nonredox" flavoenzyme. Biochemistry **43:**8652–8661.

62. **Tittmann, K.** 2009. Reaction mechanisms of thiamin phosphate enzymes: redox reactions. FEBS J. **276:**2454–2468.
63. **Trudgill, P. W.** 1984. Microbial degradation of the alicyclic ring: structural relationships and metabolic pathways, p. 131–180. *In* D. T. Gibson (ed.), Microbial degradation of organic compounds, Marcel Dekker, Inc., New York, NY.
64. **Walsh, C., et al.** 1978. Chemical and enzymatic properties of riboflavin analogues. Biochemistry **17:**1942–1951.
65. **Yoshida, K., D. Aoyama, I. Ishio, T. Shibayama, and Y. Fujita.** 1997. Organization and transcription of the *myo*-inositol operon, iol, of *Bacillus subtilis*. J. Bacteriol. **179:**4591–4598.
66. **Yoshida, K., et al.** 2008. *Myo*-inositol catabolism in *Bacillus subtilis*. J. Biol. Chem. **283:**10415–10424.
67. **Zehr, B. D., T. J. Savin, and R. E. Hall.** 1989. A one-step, low background Coomassie staining procedure for polyacrylamide gels. Anal. Biochem. **182:** 157–159.
68. **Zhang, G., J. Dai, Z. Lu, and D. Dunaway-Mariano.** 2003. The phosphonopyruvate decarboxylase from *Bacteroides fragilis*. J. Biol. Chem. **278:**41302–41308.
69. **Ziegenhorn, J., M. M. Senn, and T. Buecher.** 1976. Molar absorptivities of β-NADH and β-NADPH. Clin. Chem. **22:**151–160.